Cytotoxicity of Phosphorus Allotropes (Black, Violet, Red)

Naziah Mohamad Latiff,[a] Carmen C. Mayorga-Martinez,[b] Zdenek Sofer,[b] Adrian C. Fisher,[c] and Martin Pumera[b]*

[a] Division of Chemistry and Biological Chemistry, School of Physical and Mathematical Sciences, Nanyang Technological University, 21 Nanyang Link, Singapore 637371, Singapore

[b] Department of Inorganic Chemistry, University of Chemistry and Technology Prague, Technická 5, 166 28 Prague 6, Czech Republic

[c] Department of Chemical Engineering and Biotechnology, University of Cambridge, New Museums Site, Pembroke Street, Cambridge CB2 3RA, UK

* - author for correspondence

Keywords: cytotoxicity, black phosphorus, red phosphorus, violet phosphorus

Abstract

Black phosphorus has shown great potential in many applications such as energy, optoelectronics and bio/sensing. However, its toxicity study is still in its infancy. Here, the cytotoxicity of black phosphorus prepared by two different synthesis methods, *i.e.* vapour growth transport and high pressure conversion, are investigated. Precursor and intermediate materials, namely red and violet phosphorus, are also included in this study for a better understanding on the toxicity changes that occurs during the transformation process. We found that the cytotoxicity of phosphorus materials could be influenced by their degree of exfoliation arising from differences in morphology, as well as their extent of oxidation. These findings are important in preparing safe phosphorus materials for real life applications.

Introduction

Research on 2D layered materials continues to fascinate the scientific community with one of the latest trend showing a recent wave of publications on black phosphorus (BP). Similar to graphite, black phosphorus consists of a single element and exhibits many exciting properties as the bulk states are exfoliated into single/few-layers.[1,2] BP hold several advantages over graphene and transition metal dichalcogenides (e.g. MoS_2, $MoSe_2$, WS_2) in terms of bandgap and hole mobility. With many distinguished properties, it is not surprising that there are numerous reports on BP and its exfoliated forms displaying great potential in diverse applications ranging from ultrafast electronics, high frequency optoelectronics, telecommunications, thermal imaging, field effect transistors, photodetectors, sensing, photothermal therapy, theranostic nanomedicine, energy storage/conversion and more.[3-14] In view of their promising prospects for application in real life, it is important for us to be aware of the possible hazards they can pose to humans and the environment.[15] This is especially true for new materials such as black phosphorus where literature pertaining to their toxicological behaviour is still in its infancy.

Previously, our group had reported the toxicity of bulk BP synthesized through vapour phase growth method from red phosphorus and found it be relatively toxic.[16] The vapour phase growth method of black phosphorus is a kinetically controlled and low-pressure route from red phosphorus, with Sn/SnI_4 as a mineralization additive.[2,12] Hittorf's phosphorus, also known as violet phosphorus, has been reported as the intermediate in the vapour phase growth method.[17] To the best of our knowledge, the effect of different synthesis methods on the toxicity effects of BP has not yet been explored. With many aspects that still remain unclear pertaining to potential health hazards of these new materials, more toxicity assessments are needed.

In this report, we attempt to address this concern by studying another synthesis method of BP *via* high pressure conversion from red phosphorus (BP HPC) which is an older method and requires more energy consumption relative to the vapour phase growth method (BP VPG). In order to better understand the effect of synthesis method on the toxicity of phosphorus materials, we have also included red phosphorus (RP) and violet phosphorus (VP) in our investigation. This would enable us to track the changes in toxicity that occurs as the precursor material transforms into BP HPC and BP VPG. These materials are all allotropes of phosphorus with structures as depicted in Scheme 1.

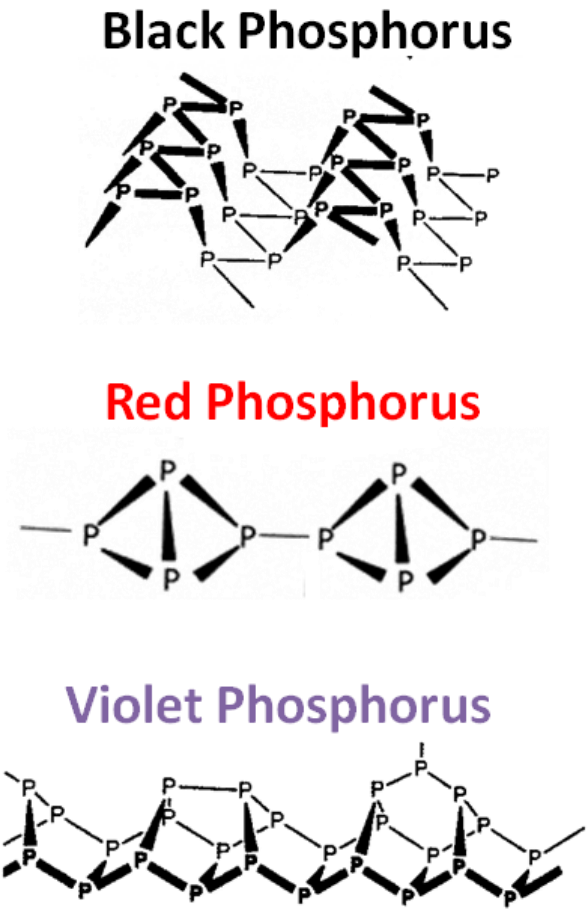

Scheme 1. Crystal structures of different P allotropes.

Human lung carcinoma epithelial (A549) cells are chosen as the respiratory tract is likely to be the first point of entry for nanomaterials through inhalation.[18-24] Upon 24 h treatment of the cells with different concentrations of the test materials, the remaining cell viability was determined using methylthiazolyldiphenyltetrazolium bromide (MTT) and water-soluble tetrazolium salt (WST-8) assays. Two assays were used to ensure reliable data. Additionally, control experiments in the absence of cells were performed to monitor for possible interferences between the phosphorus materials and the assays used.

Results and discussion

Before cytotoxicity assessment, it is important to characterize the materials first to understand their properties. The solid P allotrope materials synthesized were characterized using scanning electron microscopy (SEM) to study their morphology (Figure 1). Plate-like and distinct layered structures were observed in BP VPG while this was less clearly seen in the case of BP HPC. On the other hand, VP showed layered and ribbon-like structures whereas RP appeared like stones without observation of layered structures. Interestingly, we see different morphologies for the different phosphorus allotropes and BP materials.

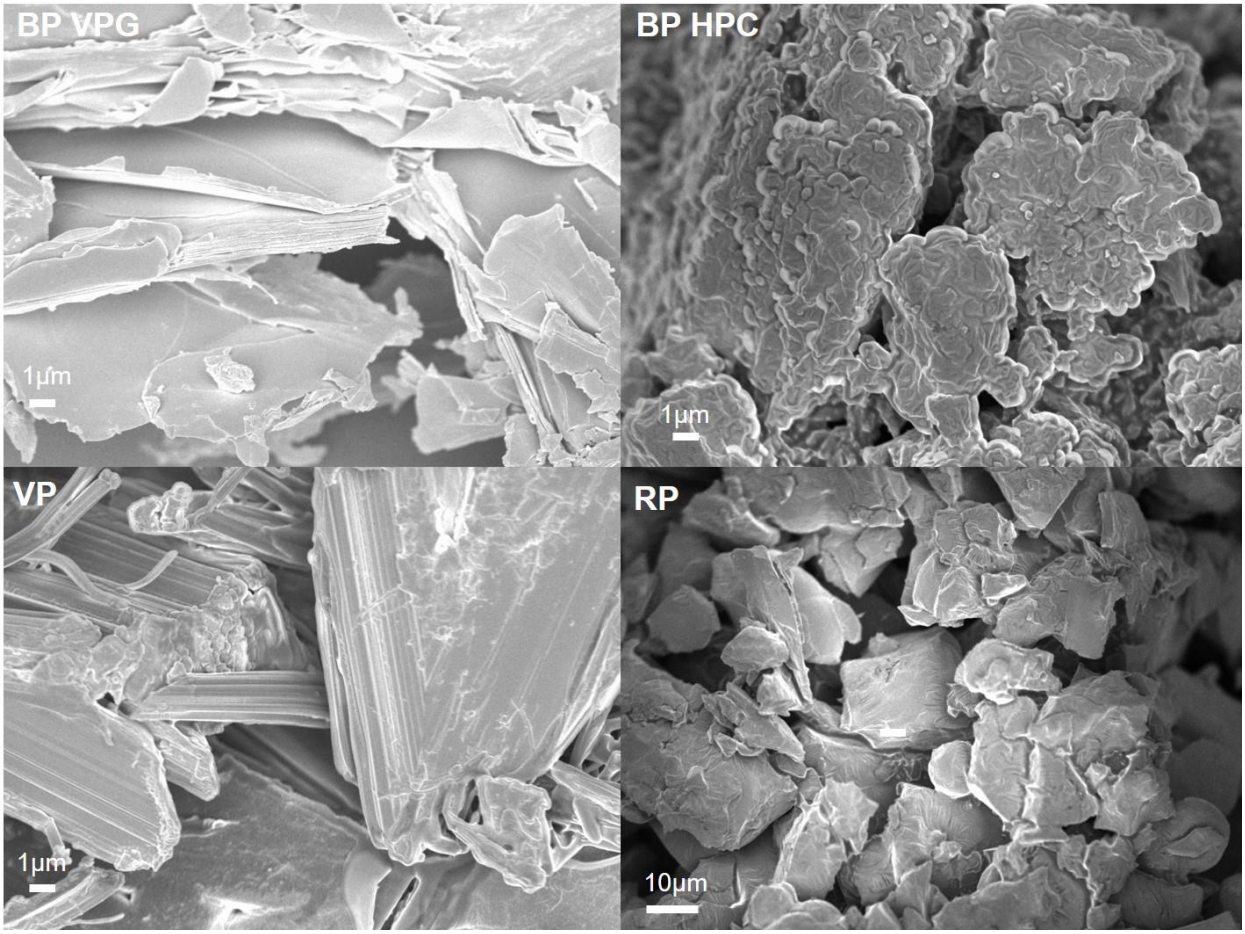

Figure 1. SEM images of black phosphorus synthesized by vapour phase growth (BP VPG), black phosphorus synthesized by high pressure conversion (BP HPC), violet phosphorus (VP) and red phosphorus (RP) used in this study.

To prepare homogenous liquid suspensions, the solid materials were dispersed in ultrapure water and sonicated for 6 h. The obtained materials were further characterized for their structure, sizes, surface charge, bonding arrangement and composition by scanning transmission electron microscope (STEM), dynamic light scattering (DLS), Raman spectroscopy and X-ray photoelectron spectroscopy (XPS).

As seen from STEM images in Figure 2, the sonication process results in exfoliation of BP VPG into few layer sheets of lateral sizes in the nano and micrometer range. However, for the other phosphorus materials, thin sheets were not observed. Instead, the materials appeared to be broken down into smaller pieces of lateral sizes in the nanometer and micrometer range.

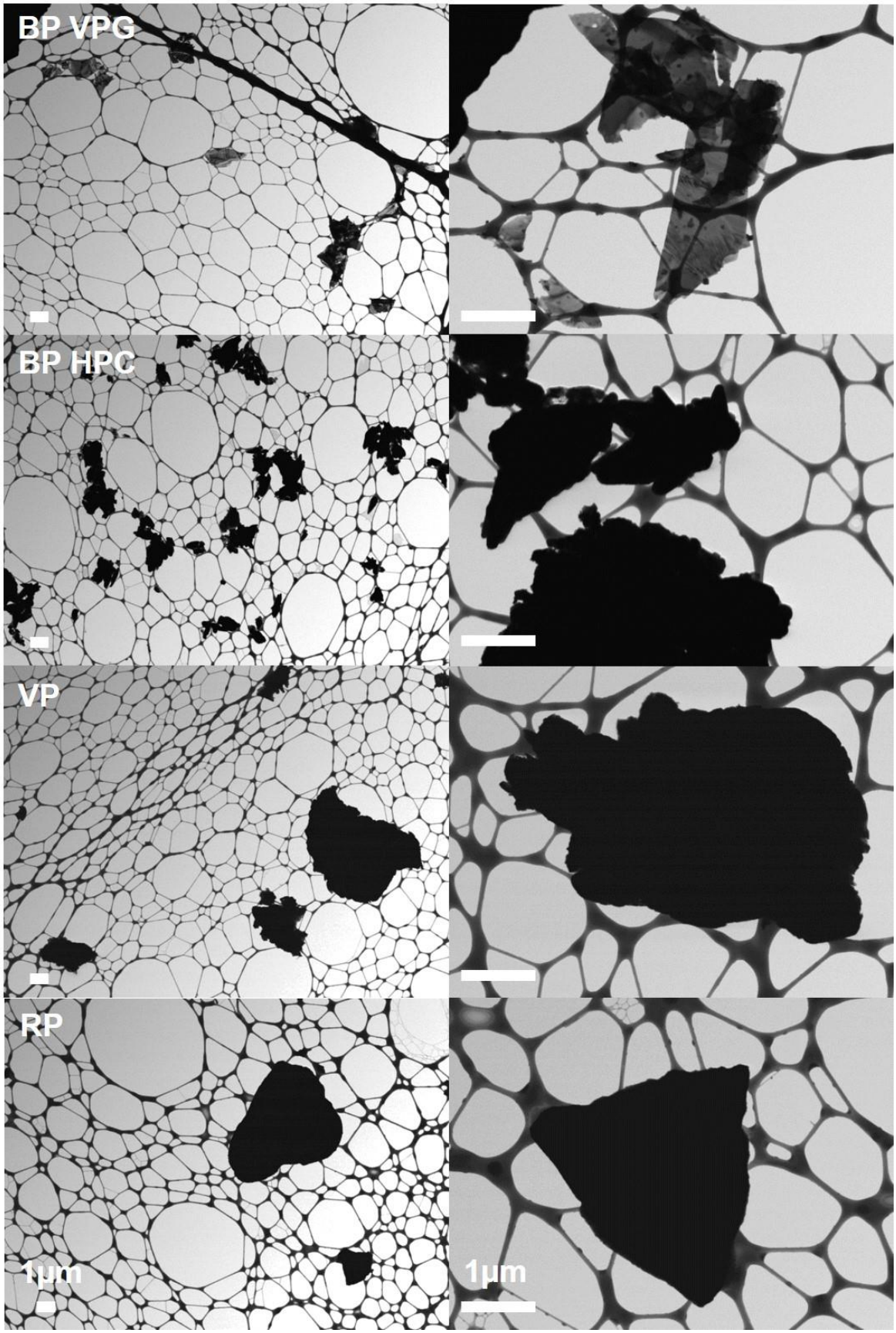
BP VPG
BP HPC
VP
RP
1μm
1μm

Figure 2. STEM images of P materials under study in low (left) and high (right) magnifications. The scale bars represent 1 μm.

Subsequently, DLS was conducted to determine the size distribution and the ζ-potential of the P materials. These parameters have been reported to influence the cytotoxicity of nanomaterials.[25] The size distribution for the P materials are as shown in the Supporting Information Figure S1. The sizes for the materials generally range between 200 nm to 1 μm. We find that the ζ- potential for all the P materials under study are close to zero (Table S1).

Following that, Raman spectroscopy was performed for the four materials evaluated in this study (Figure 3). The Raman spectra of BP VPG and BP HPC show characteristic peaks of A_{1g}, B_{2g} and A_{2g} at approximately 360 cm^{-1}, 440 cm^{-1} and 465 cm^{-1} respectively.[2,26-28] The higher intensity ratio of A_{2g} to A_{1g} modes in BP VPG (2.46 ± 0.24) relative to BP HPC (2.09 ± 0.09) suggests a decrease in number of layers as suggested from other studies.[2,29] Also, broader A_{1g}, B_{2g}, and A_{2g} peaks of BP HPC indicate larger number of layers relative to BP VPG as associated in another study[30], in agreement with the STEM results. A complex Raman spectrum of VP and RP were observed similar to previous studies.[4,31,32] The complexity arises from presence of multiple vibration modes due to low symmetry and numerous different crystallographic atoms present in the unit cell.[30]

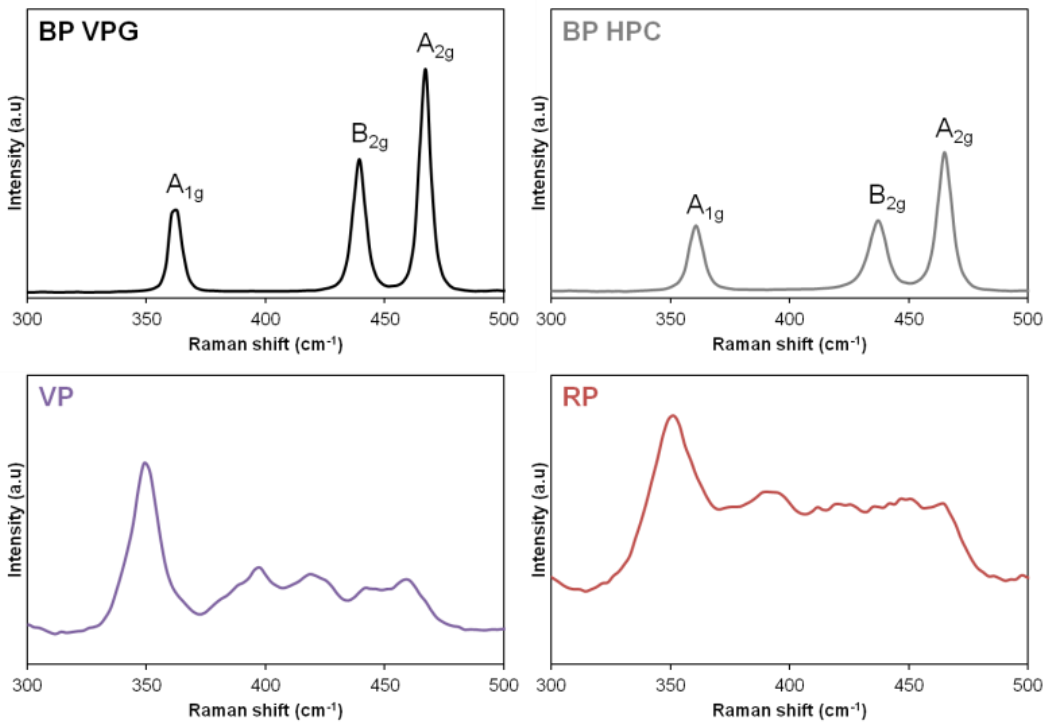

Figure 3. Raman spectra of black phosphorus synthesized by vapour phase growth (BP VPG), black phosphorus synthesized by high pressure conversion (BP HPC), violet phosphorus (VP) and red phosphorus (RP).

X-ray photoelectron spectroscopy (XPS) was later performed to analyze the composition of the phosphorus materials. Figure 4 shows the high resolution XPS spectra of the samples. Two peaks, P $2p_{3/2}$ and P $2p_{1/2}$ doublet, were seen at 129.7 ± 0.6 eV and 130.6 ± 0.6 eV respectively which are characteristic peaks of crystalline BP.[33] An oxidized phosphorus (PO_X) peak is apparent at 134 ± 0.6 eV which could be formed through oxidation in water and ambient conditions.[34] The different samples show varying amounts of oxidations in comparison with the P 2p peaks.

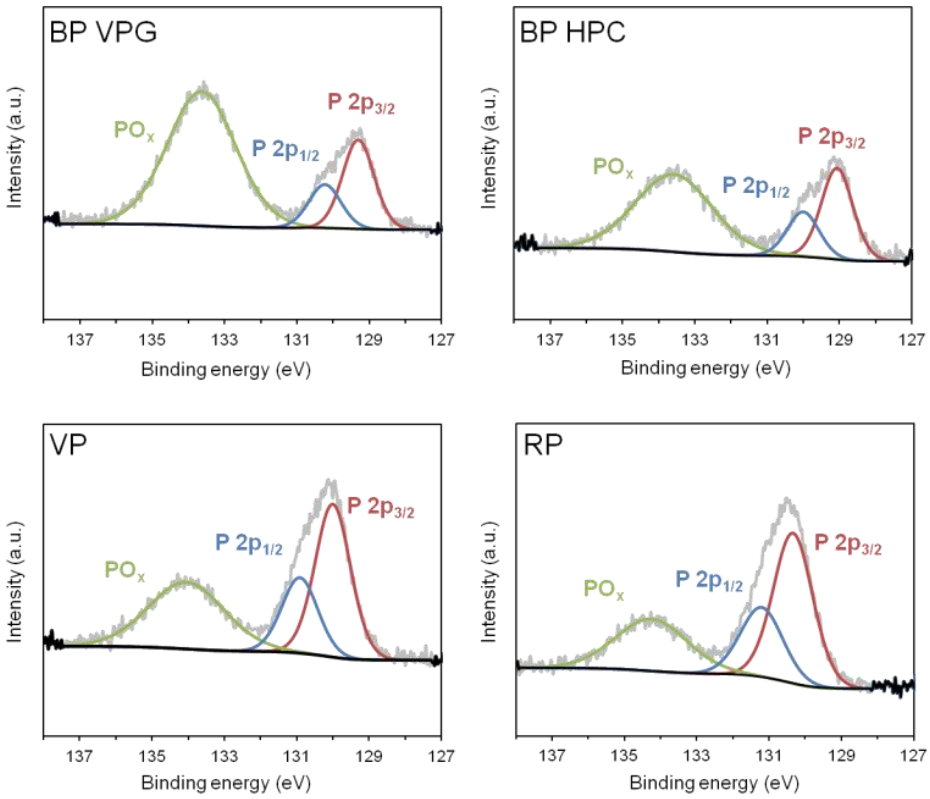

Figure 4. High resolution P 2p X-ray photoelectron spectroscopy (XPS) spectra of the materials under study: black phosphorus synthesized by vapour phase growth (BP VPG), black phosphorus synthesized by high pressure conversion (BP HPC), violet phosphorus (VP) and red phosphorus (RP).

To observe this difference better, we calculated the ratio of areas under the PO_X to the sum of P 2p peaks (i.e. PO_X/P ratio) and presented them in Table 1 below. Among the P allotropes studied here, the two BP materials show higher contents of PO_X compared to VP and RP. Between BP VPG and BP HPC, we found BP VPG to have higher amounts of oxidized PO_X species.

Table 1. Comparison for ratio of oxidized phosphorus (PO_X) to phosphorus determined from XPS deconvolution of high resolution spectrum of P 2p core level for black phosphorus

synthesized by vapour phase growth (BP VPG), black phosphorus synthesized by high pressure conversion (BP HPC), violet phosphorus (VP) and red phosphorus (RP).

P material	PO_X/P ratio
BP VPG	1.09
BP HPC	0.70
VP	0.31
RP	0.21

To further support the trends seen for oxidation of the different phosphorus allotropes, we studied the intrinsic redox properties of the materials using cyclic voltammetry (CV) in N_2 purged 50 mM phosphate buffer solution (PBS, pH 7.2). The recorded CVs in anodic and cathodic direction for phosphorus allotropes were shown in Figure 5. The BP VPG and BP HPC show an oxidation peak around 0.5 V that corresponds to the oxidation of P^0 to P^{5+}.[35, 36]

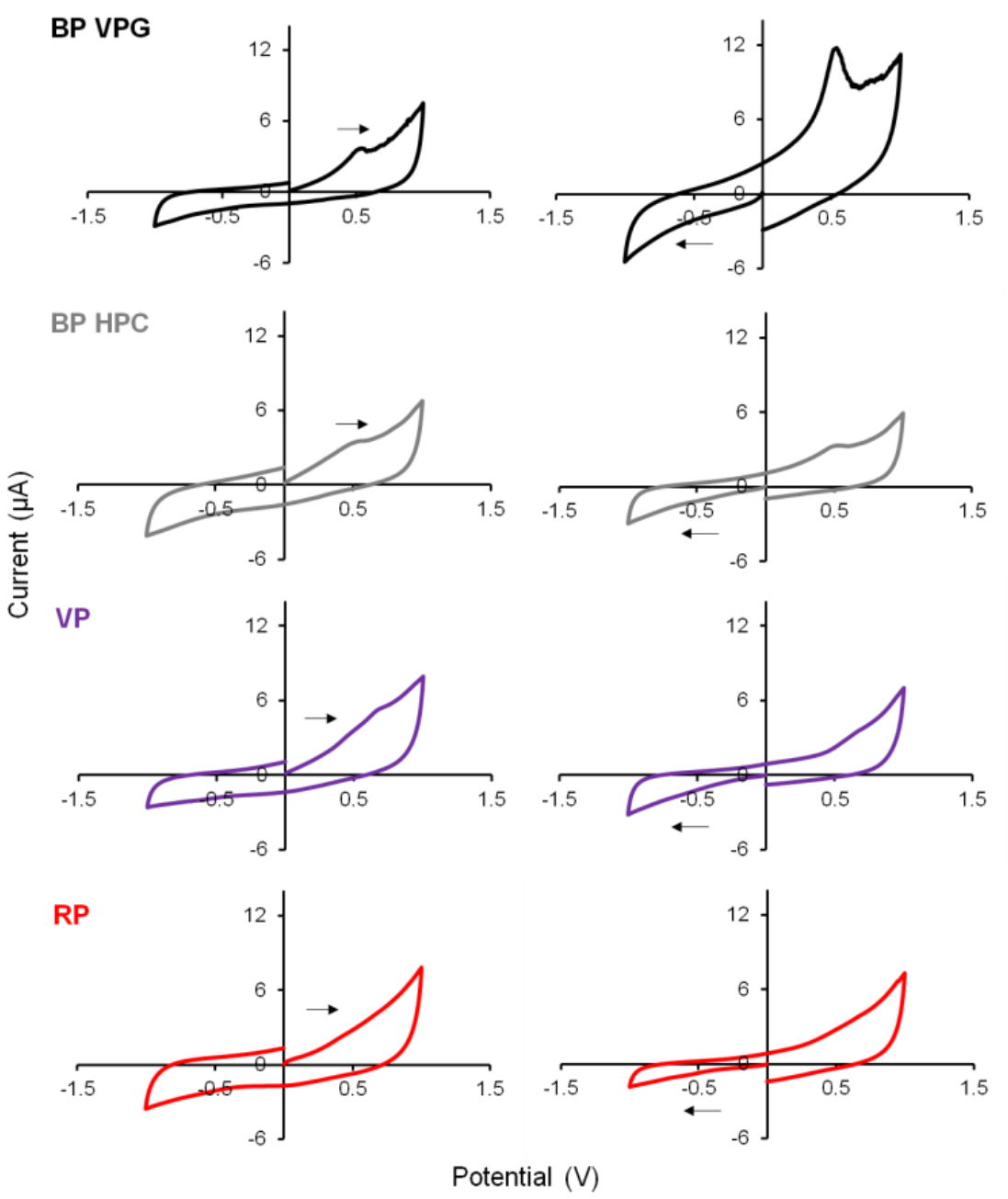

Figure 5. Inherent electrochemistry of black phosphorus synthesized by vapour phase growth (BP VPG), black phosphorus synthesized by high pressure conversion (BP HPC), violet phosphorus (VP) and red phosphorus (RP) performed in the anodic direction (left) and cathodic direction (right). Conditions used: 50 mM phosphate buffer solution (PBS) pH 7.2 at a scan rate of 100 mV/s. The arrows indicate the scan direction.

Interestingly in the case of BP VPG, the intensity of the oxidation peak enhances if the CV was recorded in cathodic direction. This was not seen in BP HPC, and this is in good agreement with the XPS data which showed BP VPG having higher surface oxidation compared to BP HPC. In this way, the high pressure conversion method used for synthesizing BP enhance the stability and decrease the passivation observed in BP synthesized by vapour phase growth after the sonication process.

After material characterization, we proceeded to toxicity investigation. In our previous study, BP was found to interfere with the WST-8 and MTT assay by reducing the active tetrazolium salts reagents to the formazan products which are generated by metabolically active cells, thereby giving to false negative results.[16] Also, MTT assay can bind with the formazan crystal produced to cause overestimation of cell viability readings. To minimize these interferences, washing steps with PBS were implemented in that study to remove the phosphorus materials prior to addition of the cell viability assay reagents.

Here, we modified the previous method to minimize these nanomaterial-induced effects by studying the lower concentration range (3.125 to 25 μg/ml) where the interference effects are comparably smaller (see Figure 6). These control experiments were carried out by incubating the phosphorus materials with the MTT and WST-8 assay in the absence of cells. Data was normalized with a blank control which does not contain any phosphorus materials. At these low concentration range, the percentage of control formazan produced was reduced significantly to below 200% as compared to 800% as seen from our previous study for BP VPG (tested between 3.125 to 400 μg/ml).

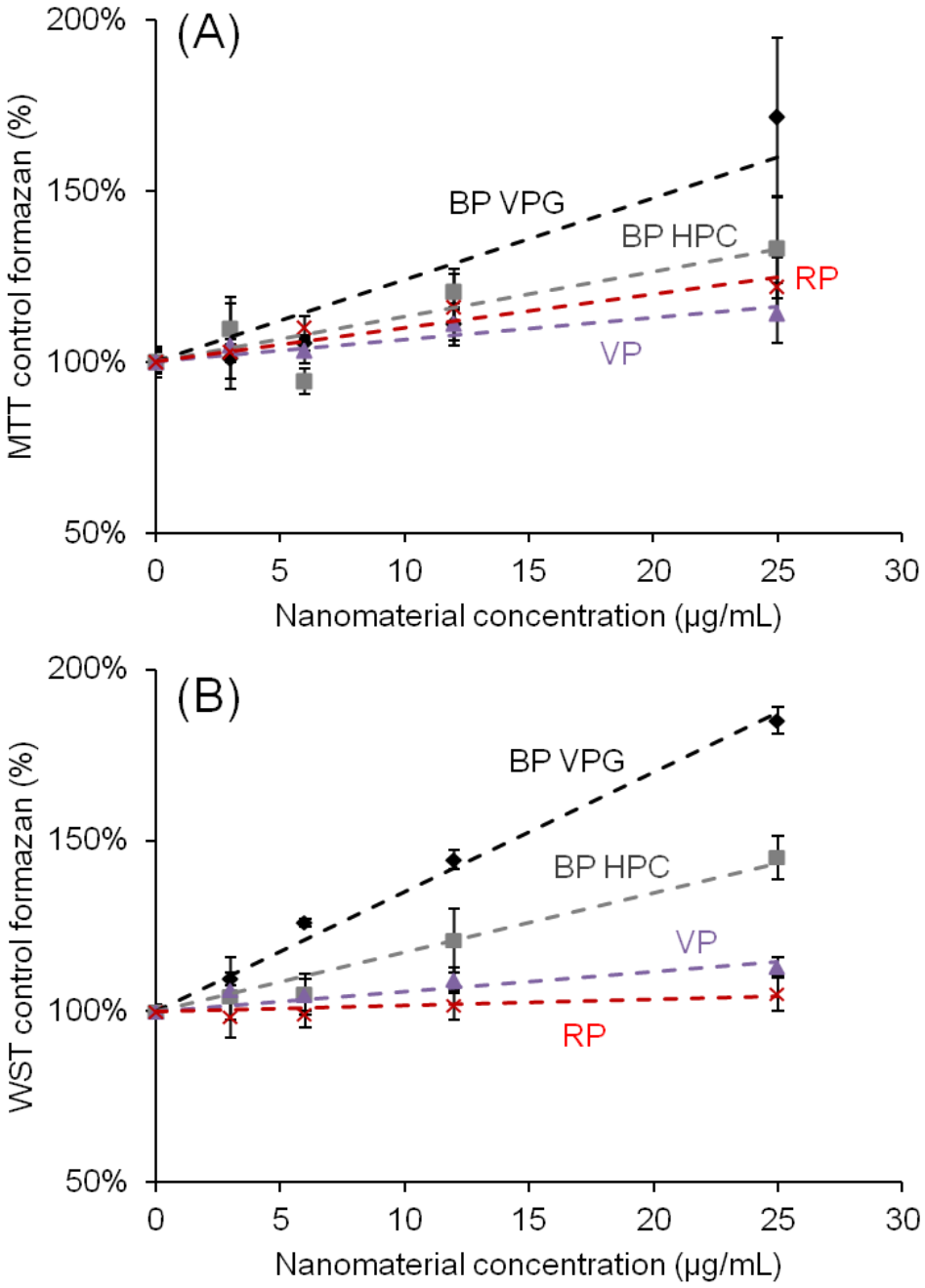

Figure 6. Control experiments (in the absence of cells) to check for interferences between (A) MTT and (B) WST-8 cell viability assays with black phosphorus synthesized by vapour phase growth (BP VPG), black phosphorus synthesized by high pressure conversion (BP HPC), violet phosphorus (VP) and red phosphorus (RP).

Moreover, for a more accurate analysis, we used the data obtained from control experiments as a blank subtraction for analyzing the results collected from experiments with cells. This would enable us to reduce any nanomaterial-induced interference including possible binding interaction between nanomaterials with MTT formazan crystals for the cytotoxicity evaluation.

Using these modifications to the previous method, results from the cytotoxicity assessment (Figure 7) reveal that BP VPG has higher toxicity compared to BP HPC. To illustrate, BP VPG had *ca.* 20-30% lower viable cells than BP HPC upon 25 μg/ml BP tested using both MTT and WST-8 assays, despite its greater ease while sharing the same precursor (RP). Interestingly starting precursor material (RP) show relatively low toxicities with cell viability values remaining above 75% upon 24 h treatment of 25 μg/ml RP. These trends are in agreement for both the MTT and WST-8 assay. These finding suggest that the toxicity of BP is contributed by synthesis processes involved during the conversion from RP to BP HPC and BP VPG. To confirm this assertion, another allotrope VP that is an intermediate material for BP synthesized by vapour phase growth synthesis was studied as well. This P allotrope shows low toxicities with cell viability values remaining above 70% upon 24 h treatment of 25 μg/ml VP, demonstrating that the higher toxicity of BP VPG is not related to the toxicity of VP. In view of the different reagents involved during the synthesis process of BP VPG and BP HPC, one may think that SnI_4 introduced through the vapour growth phase synthesis method could possibly contribute to the higher toxicity of BP VPG. However, the synthesis method of VP also involves SnI_4 and yet we found VP to be a relatively safe material. This hints that there are other factors apart from metal content which play a greater role in influencing the toxicity of these phosphorus materials.

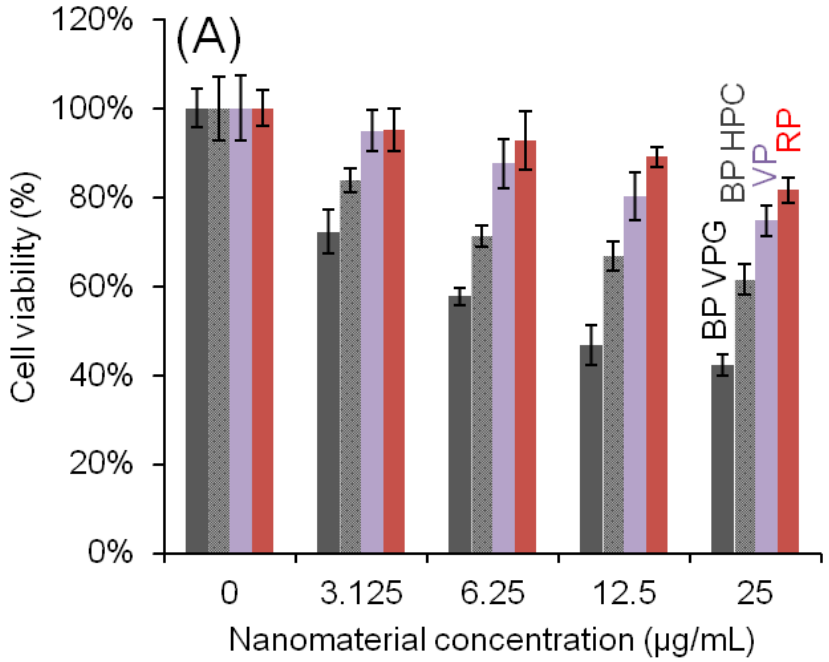
(A)
120%
100%
80%
60%
40%
20%
0%
Cell viability (%)
BP VPG
BP HPC
VP
RP
0
3.125
6.25
12.5
25
Nanomaterial concentration (μg/mL)

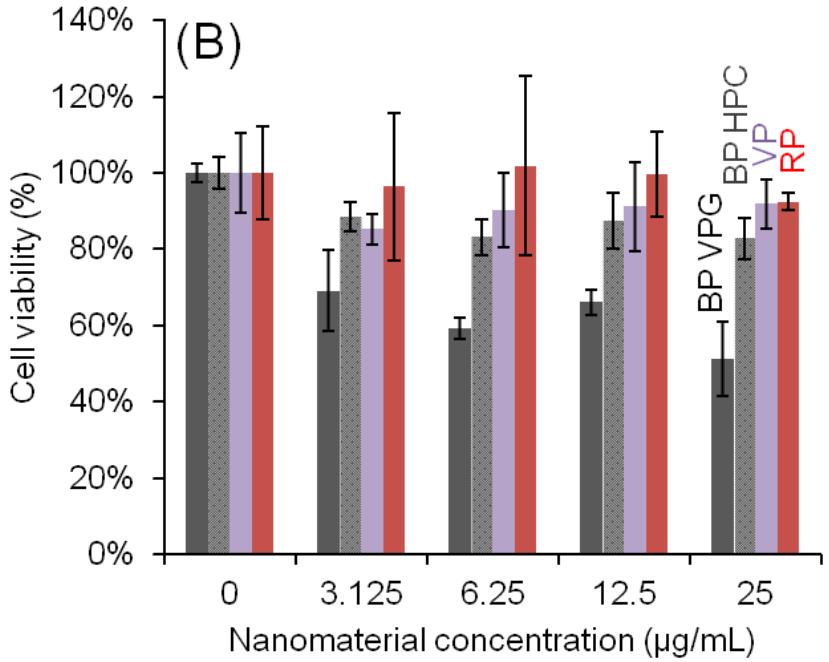
(B)
140%
120%
100%
80%
60%
40%
20%
0%
Cell viability (%)
BP VPG
BP HPC
VP
RP
0
3.125
6.25
12.5
25
Nanomaterial concentration (μg/mL)

Figure 7. Cytotoxicity assessment of black phosphorus synthesized by vapour phase growth (BP VPG), black phosphorus synthesized by high pressure conversion (BP HPC), violet phosphorus (VP) and red phosphorus (RP) using (A) MTT assay and (B) WST-8 assay.

To further verify our results, we also performed staining of the live and dead cells using calcein and ethidium homodimer respectively, after treatment with the P materials (Figure 8). We found a similar trend where BP VPG shows the highest ratio of dead to live cells, followed by BP HPC and VP, while RP shows the lowest ratio of dead/live cells.

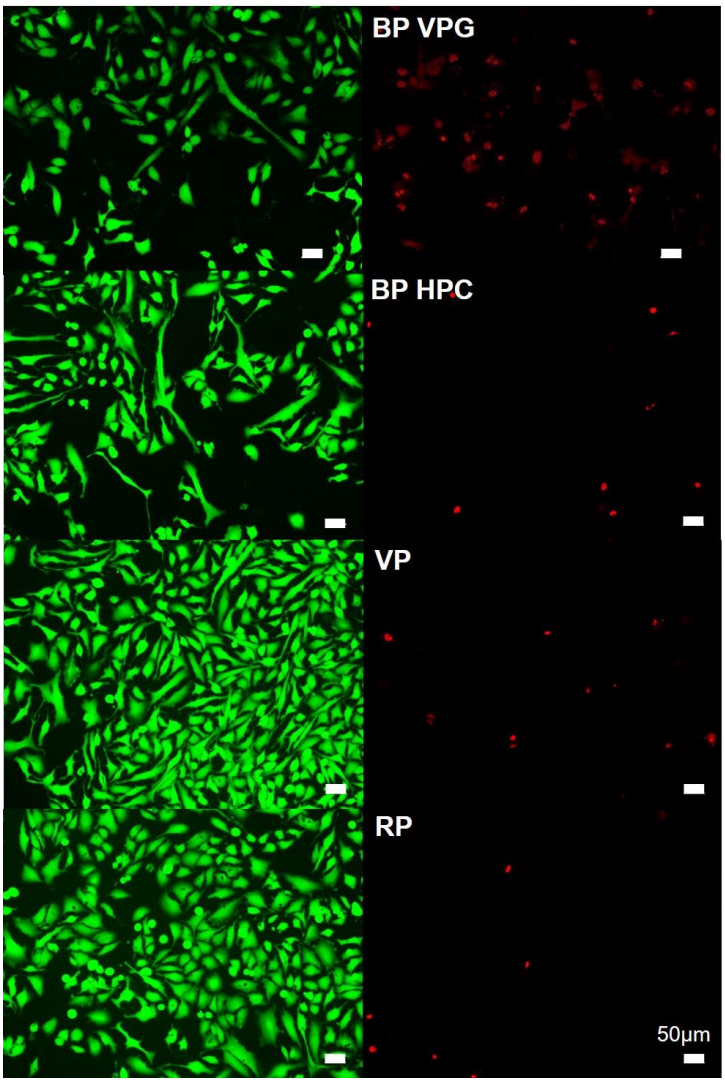

Figure 8. Live/Dead staining of A549 cells after 24 h exposure to 25 μg/ml of the various P materials under study. Live cells were stained green using calcein while dead cells were stained red using ethidium homodimer. The scale bars represent 50 μm.

Comparing the trend of toxicological behaviour towards A549 cells with the material characterization results, there appears to be a correlation between a higher degree of exfoliation and higher PO_X/P content to higher toxicity of phosphorus materials. The differences in degree of exfoliation is likely to arise from differences in morphology of the materials. BP VPG shows distinct layered structures from SEM imaging (see Figure 1) unlike the other phosphorus materials studied. Here, it is important to highlight that only BP VPG shows exfoliated nanosheets structures after the sonication process (see Figure 2 and Figure S1). It is well known that liquid phase exfoliation method oxidizes and degrades BP.[35] However, thinner sheets of layered materials has been reported to have increased toxicological effects.[36]

The correlation between toxicity and oxidation degree is similar to a previous report on cytotoxicity of graphene oxide (GO) prepared by different oxidation methods used *i.e.* Staudenmaier, Hummers, Hoffman and Tours methods. In that study, Chng *et al.* found that cytotoxicity of the GO materials was influenced by their C/O ratios and C=O contents.[37] The Hummers and Tours oxidation methods, which involved permanganate treatment, result in a greater extent of oxidation and produced GO materials with a stronger toxic effect on the A549 cells. On the other hand, the Staudenmaier and Hoffman oxidation methods, which involved chlorate treatment, produced GO materials with lower oxygen contents and lower toxicities. This similarity is interesting as both graphite and black phosphorus are layered materials that consist of only one element, unlike other layered materials such as transition metal dichalcogenides.

Moreover, a higher oxidative activity seen from inherent electrochemistry analysis could indicate higher potential for the material to produce oxygen radicals. This has been associated in a previous study which found ZnO nanoparticles to have higher chemical activity relative to silicon oxide nanoparticles and resulted in higher levels of oxidative stress produced.[38] With many *in vitro* studies of BP reporting the production of reactive oxygen species (ROS) as a mechanism to induce apoptosis, the higher chemical activity of BP VPG particles is likely to be the reason for its higher cytotoxicity behaviour observed.[39,40]

To ascertain whether the mechanism for cell death is by ROS production, we measured the ratio of the reduced to oxidized forms of glutathione (GSH/GSSG). A decrease in GSH/GSSG ratio has been widely reported to be a useful indicator for oxidative stress.[41] We found this value to decrease from 65 for the negative control (without test materials) to 11, 13, 19 and 26 after exposure to 25 μg/ml of BP VPG, BP HPC, VP and RP respectively (Figure 9). This trend correlates well with the toxicity results obtained in Figure 7, thereby suggesting that the generation of ROS is a cause for cell death induced by the P materials.

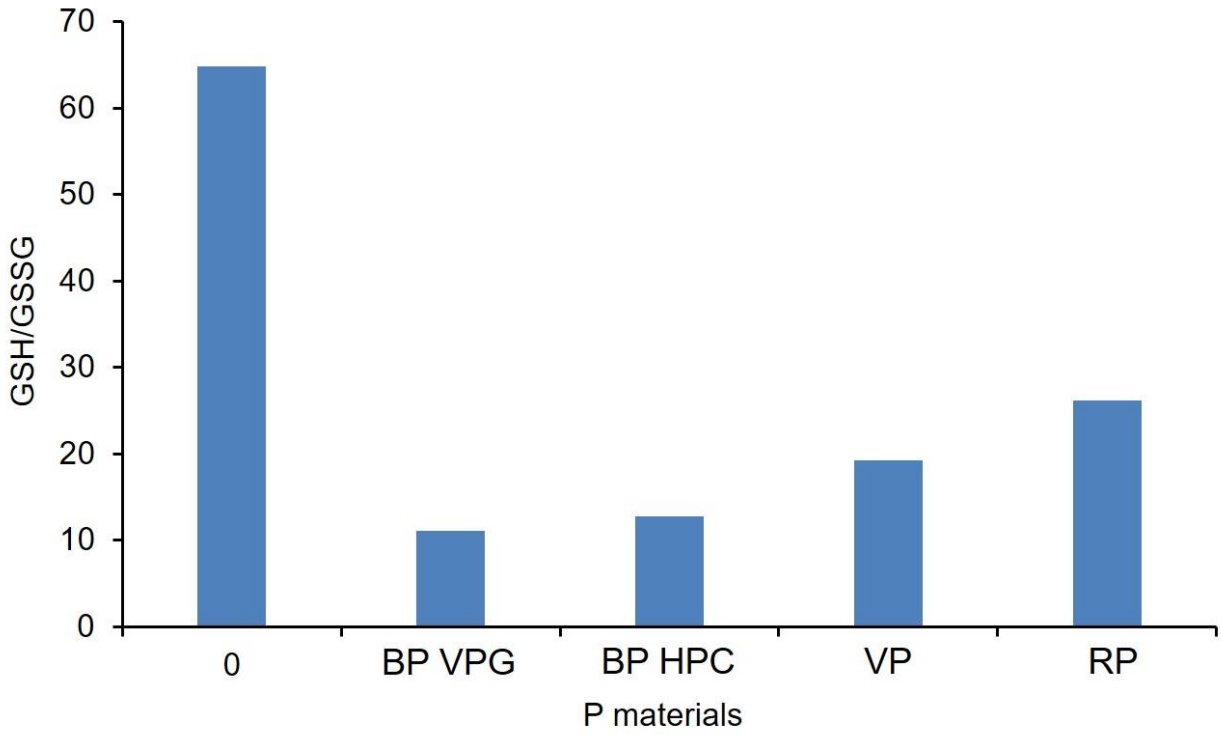

Figure 9. GSH/GSSG ratio determined for A549 cells after 24 h treatment with 25 μg/ml of different P materials.

Apart from finding a mechanism for cell death, we also investigated the cell apoptosis process using a real-time assay that measures the presence of phosphatidylserine on the outer layer of cell membranes during apoptosis, through binding of annexin V which produces a luminescence signal. Necrosis process was also detected concurrently using a cell-impermeant fluorescent DNA dye for simultaneous real-time monitoring of apoptotic progression. The results as shown in Figure 10 revealed signs of early apoptosis when A549 cells were treated with 25 μg/ml of the different P allotrope materials, as evident from the increase in luminescence signal while the fluorescence signal remains low.

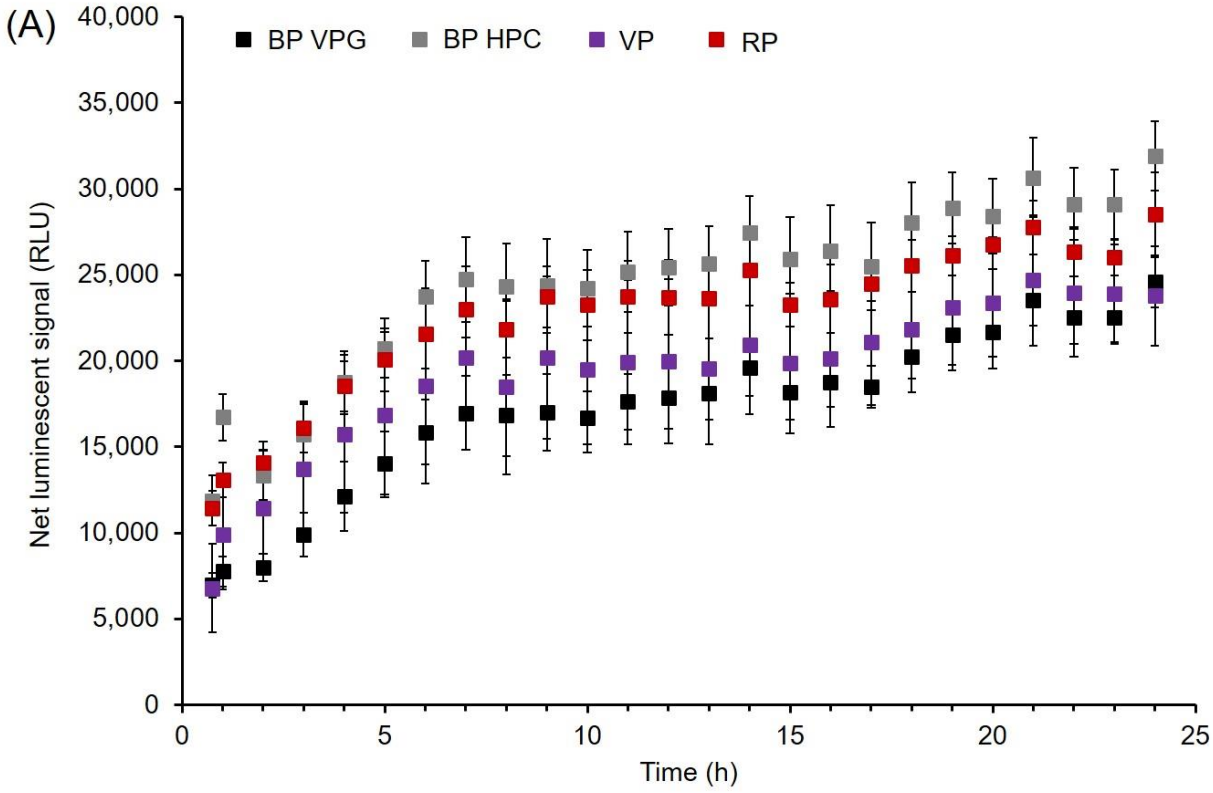
(A)
BP VPG
BP HPC
VP
RP
Net luminescent signal (RLU)
40,000
35,000
30,000
25,000
20,000
15,000
10,000
5,000
0
0
5
10
15
20
25
Time (h)

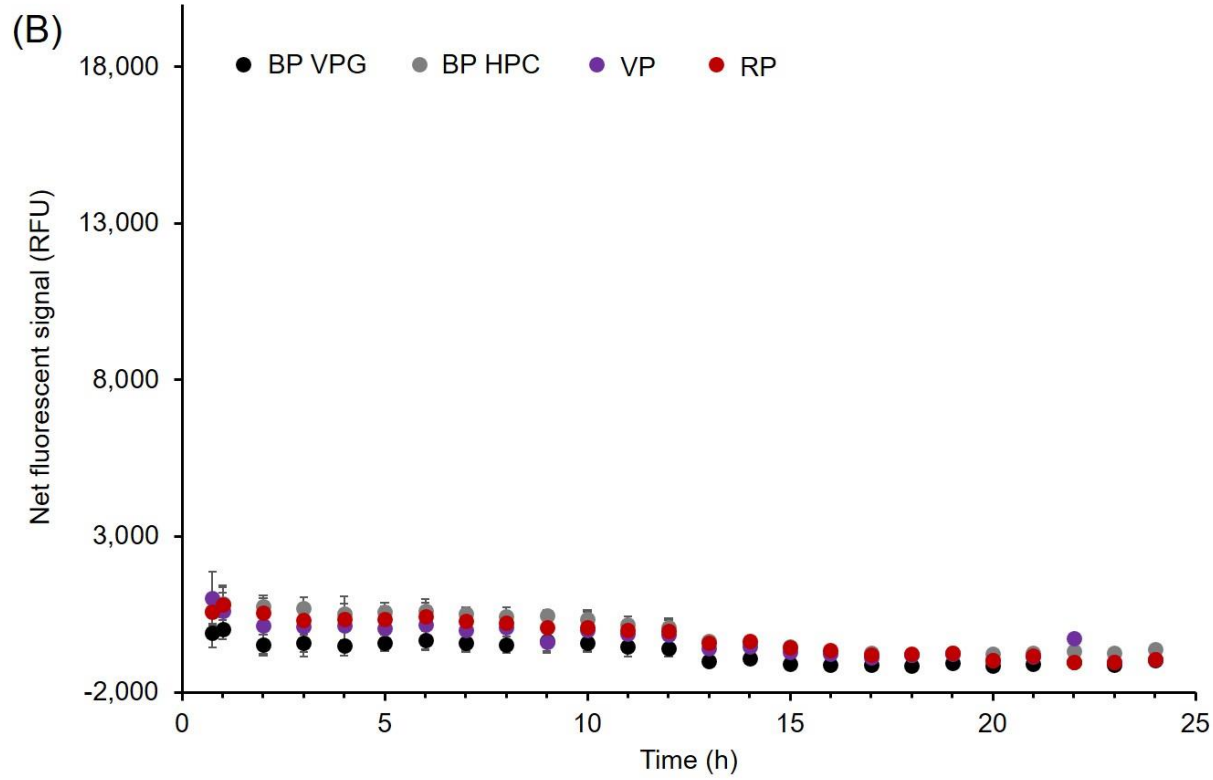
(B)
BP VPG
BP HPC
VP
RP
Net fluorescent signal (RFU)
18,000
13,000
8,000
3,000
-2,000
0
5
10
15
20
25
Time (h)

Figure 10. Real-time monitoring of net luminescent (A) and fluorescent (B) signals measured for A549 cells treated with 25 μg/ml of BP VPG, BP HPC, VP and RP over 24 hours, reported in relative luminescence units (RLU) and relative fluorescence units (RFU) respectively .

Besides A549 cells, we have also tested the P materials with other cell lines such as human embryonic kidney cells (HEK293), human cervical carcinoma cells (HeLa), human breast cancer cells (MCF7) and human liver carcinoma cells (HepG2) with WST-8 assay to extend the scope of this study (see Supporting Information Figure S2). Interestingly, we did not find a similar trend as seen for A549. This may be due to different sensitivities of the different cell lines.

We compared our data here with our previous work of other layered materials tested under similar conditions (Table 2). However, it should be noted that the degree of exfoliation varies for the different samples depending on the exfoliation method used and the interlayer distance between layers of the material. It has been reported by several studies that size, thickness, shape, oxygen content, surface charges and elements of nanomaterials can greatly influence the toxicological property of nanomaterials.[36,37,40,42-45] The large number of possible factors that can vary makes good comparison between different reports challenging. Further and systematic studies have to be conducted to further elucidate this evaluation. Generally, our finding shows that BP can have large differences in toxicity depending on the synthesis method used.

Table 2. Comparison of cytotoxicity of nanomaterials using WST-8 assay for cell viability measurement upon treatment of 25 μg/ml of material for 24 h. GO-HU represents graphene oxide synthesized by Hummers oxidation method. Hummers oxidation method is chosen over the other methods as it is the more commonly used oxidation method seen in literature.[46,47]

Material	Cell viability (%)	Reference
BP VPG	51	This work
BP HPC	83	This work
VP	92	This work
RP	92	This work
GO-HU	60	37
MoS_2	78	36

Conclusion

With rising interest in research on allotropes of phosphorus, especially for black phosphorus, there is great possibility of these materials entering the commercial in the future. However, as new materials, more studies are required to better understand the toxicological effects of black phosphorus. Here, we investigated the cytotoxicity of black phosphorus synthesized by vapour phase growth and high pressure conversion, as well as their precursor red phosphorus. The intermediate for vapour phase growth synthesis method, violet phosphorus, was also included for a more complete study. We found black phosphorus synthesized by vapour growth transport to have higher toxicity effects compared to black phosphorus produced *via* high pressure conversion. In comparison with black phosphorus, red and violet phosphorus show relatively low toxicities. Even though both black and violet phosphorus were synthesized from red phosphorus, they have significantly different toxicities. These findings demonstrate how synthesis methods can greatly influence the properties of the BP materials produced as well as its toxicological effects. We find that the toxicity of phosphorus materials is likely to be influenced by their degree of exfoliation and extent of oxidation. BP VPG with thinner sheets was observed to be

more toxic compared to BP HPC with thicker structures. Furthermore, our results showed that phosphorus materials with higher content of oxidation resulted in higher toxicity profiles. This preliminary study advances our understanding pertaining to toxicity of phosphorus materials to prepare for their actual commercialization in real life.

Experimental Section

Synthesis of different P allotropes

The materials were synthesized as follows:[34]

Black phosphorus materials were prepared by vapour phase growth (BP VPG) and high pressure conversion (BP HPC). For the former method (BP VPG), 500 mg of Au/Sn alloy, 15 mg SnI_4 and 720 mg of red phosphorus were placed in a quartz ampoule and sealed using an oxygen/hydrogen torch. The Au/Sn alloy was prepared by melting stoichiometric amounts of tin (Sigma Aldrich, Czech Republic) and gold (Safina, Czech Republic) under high vacuum while SnI4 was prepared by refluxing iodine (Penta, Czech Republic) and tin in chloroform (Penta, Czech Republic), and purification by recrystallization from chloroform. Following that, the ampoule was heated using a muffle furnace to 400 ^{o}C for 1 h and then left at these conditions for another two hours. Subsequently, the temperature was raised to 600 ^{o}C for one day (24 h) and cooled overnight to room temperature. The BP plates formed were washed with CS_2 (Penta, Czech Republic) to remove traces of white phosphorus produced during synthesis. For the latter method (BP HPC), 10 g of red phosphorus (Sigma Aldrich, Czech Republic) was wrapped in graphite foil and pressurized to 6 GPa and heated to 600 ^{o}C. Later, the product was cooled slowly to room temperature and removed from the graphite foil mechanically.

For violet phosphorus, it was synthesized by vapour transport of 1 g of red phosphorus (Sigma Aldrich, Czech Republic) with 40 mg of Sn and 20 mg of SnI_4 in a quartz glass ampoule. The ampoule was then placed in a muffle furnace for heating to 600 ºC, at a heating rate of 5 ºC/min. After 24 h, it was then cooled to room temperature at a cooling rate of 1 ºC/min. Violet phosphorus was produced in the middle part of the ampoule while mixture of violet and black phosphorus was formed at the end of the ampoule. The product was washed with CS_2 to remove traces of white phosphorus produced during synthesis.

To prepare their liquid suspensions, the solid materials were dispersed in ultrapure water to achieve a concentration of 1 mg/ml and sonicated for 6 h to obtain well-dispersed solutions.

Characterization

Size and morphology characterization of phosphorus allotropes were conducted by SEM and STEM using JOEL 7600F. The DLS size and surface zeta potential measurements were performed at room temperature (20°C) using clear disposable zeta cells. Chemical composition was characterized using XPS (Phoibos 100 spectrometer, SPECS, Germany) with a monochromatic Mg X-ray radiation source. Raman analysis was performed by LabRam HR instrument (Horiba Scientific).

Inherent electrochemisty studies were conducted by cyclic voltammetry measurements using compact and modular potentiostat/glavanostat (Autolab PGSTAT204/FRA32M, Eco Chemie, Utrecht, Netherlands) at a scan rate of 100 mV/s. A three electrode configuration composed of a Pt counter electrode, glassy carbon working electrode and Ag/AgCl reference electrode was used. The bare glassy carbon working electrode was modified with 0.0015 mg of test material by drop-cast method.

MTT control experiment

Cell-free MTT control experiments were conducted in a similar manner as that for WST-8. However, in this case, 1 mg/ml MTT assay was used, the reaction mixtures were incubation for 3 h and the absorbance readings were measured at 570 nm.

WST-8 control experiment

For cell-free WST-8 control experiments, different concentrations of MPX_Y suspensions were incubated with 10 % WST-8 assay in cell culture media for 1 h. Thereafter, the absorbance reading was measured at 450 nm. The results were normalized with a blank control which was not subjected to any test materials.

Cell culture

A549 human lung carcinoma epithelial cells (PAA laboratories), HEK293, HeLa, MCF7, HepG2 (ATCC) were cultured in DMEM (Dulbecco's modified eagle medium, Life Technologies) supplemented with 10 % FBS (foetal bovine serum, Life Technologies) and 1 % penicillin/streptomycin (Capricorn). The cells were incubated at 37 ^{o}C under 5 % CO_2 atmosphere.

Exposure of cells to test materials

Cells were seeded on 96 well plates (5000 cells/well) for 24 h. Following that, the cell culture media was removed and replaced with different concentrations of material suspensions in cell culture media (0, 3.125, 6.25, 12.5, 50, 100 μg/mL; 100 μl/well). A set of positive control

containing 10 % DMSO (dimethyl sulfoxide, Tedia) was prepared for every set of experiment to check on the vitality of the cells used.

Cytotoxicity assessment

Following 24 h exposure of the A549 cells to varying concentrations of material suspensions, MTT (Sigma Aldrich) and WST-8 (Dojindo) cell viability assays were conducted. In the case of MTT assay, the solutions were removed from the wells and 100 µl of 1 mg/ml MTT stock solution were added to each well. For WST-8 assay, 10 µl of WST-8 assay was added directly to each well after the exposure with test materials. Following addition of WST-8 assay, the plates were wrapped in Aluminium foil and incubated at 37ºC and 5% CO_2 for 1h before absorbance measurement at 450 nm. In the case of MTT, the incubation period was 3 h and the absorbance measurement was performed at 570 nm. Absorbance readings obtained from a corresponding set of control experiments were subtracted away from the absorbance readings obtained from wells with cells. Results from these readings were then normalization with the negative control which was not subjected to any test materials.

Live and dead cells were stained using 1 µM calcein and 2 µM ethidium bromide from Life Technologies, after treatment of the A549 cells with the P materials. Upon 45 min incubation of the cells with the dye, the live and dead cells were viewed under Nikon fluorescent microscope at 485/530 nm and 530/645 nm respectively.

Mechanistic studies

GSH/GSSG and apoptosis/necrosis real-time monitoring were determined using GSH/GSSG-Glo Assay and RealTime-Glo™ Annexin V from Promega following the instructions provided.

ASSOCIATED CONTENT

The Supporting Information contains results obtained from DLS for the P materials under study as well as the cytotoxicity assessment of these materials with other cell lines.

ACKNOWLEDGMENT

M.P., A.C.F. and N.M.L acknowledge the Singapore's National Research Foundation (NRF) under its Campus for Research Excellence and Technological Enterprise (CREATE) programme for funding. N. M. L. appreciates the RealTime-Glo™ Annexin V Apoptosis and Necrosis Assay sample from Promega. Z.S. thanks the Czech Science Foundation (GACR No.15-09001S) and by specific university research funding (MSMT No. 20-SVV/2017).

ABBREVIATIONS

BP, black phosphorus; VP, violet phosphorus; RP, red phosphorus; WST-8, water-soluble tetrazolium salt.

REFERENCES

1. Gusmão, R.; Sofer, Z.; Pumera, M. Black Phosphorus Rediscovered: From Bulk Material to Monolayers. *Angew. Chem. Int. Ed.* **2017**, *56*, 8052–8072.

2. Eswaraiah, V.; Zeng, Q.; Long, Y.; Liu, Z. Black phosphorus nanosheets: synthesis, characterization and applications. *Small* **2016**, *12*, 3480–3502.

3. Bagheri, S.; Mansouri, N.; Aghaie, E. Phosphorene: a new competitor for graphene. *Int. J. Hydrogen Energy* **2016**, *41*, 4085–4095.

4. Ma, Y.; Shen, C.; Zhang, A.; Chen, L.; Liu, Y.; Chen, J.; Liu, Q.; Li, Z.; Amer, M. R.; Nilges, T.; Abbas, A. N.; Zhou, C. Black Phosphorus Field-Effect Transistors with Work Function Tunable Contacts. *ACS Nano* **2017**, *11*, 7126−7133.

5. Shao, J.; Xie, H.; Huang, H.; Li, Z.; Sun, Z.; Xu, Y.; Xiao, Q.; Yu, X.-F.; Zhao, Y.; Zhang, H.; Wang, H.; Chu, P. K. Biodegradable black phosphorus-based nanospheres for *in vivo* photothermal cancer therapy. *Nat. Commun.* **2016**, *7*, 12967.

6. Qian, X.; Gu, Z.; Chen, Y. Two-dimensional black phosphorus nanosheets for theranostic nanomedicine. *Mater. Horiz.* **2017**, *4*, 800–816.

7. Ling, X.; Wang, H.; Huang, S.; Xia, F.; Dresselhaus, M. S. The renaissance of black phosphorus. *Proc. Natl. Acad. Sci. U. S. A*. **2015**, *112*, 4523–4530.

8. Mayorga-Martinez, C. C.; Latiff, N. M.; Eng, A. Y. S.; Sofer, Z.; Pumera, M. Black Phosphorus Nanoparticle Labels for Immunoassays via Hydrogen Evolution Reaction Mediation. *Anal. Chem.* **2016**, *88*, 10074–10079.

9. Li, P.; Zhang, D.; Liu, J.; Chang, H.; Sun, Y.; Yin, N. Air-Stable Black Phosphorus Devices for Ion Sensing. *ACS Appl. Mater. Interfaces* **2015**, *7*, 24396–24402.

10. Abbas, A. N.; Liu, B.; Chen, L.; Ma, Y.; Cong, S.; Aroonyadet, N.; Köpf, M.; Nilges, T.; Zhou, C. Black Phosphorus Gas Sensors. *ACS Nano* **2015**, *9*, 5618–5624.

11. Mayorga-Martinez, C. C.; Sofer, Z.; Pumera, M. Layered Black Phosphorus as a Selective Vapor Sensor. *Angew. Chem. Int. Ed.* **2015**, *54*, 14317–14320.

12. Sajedi-Moghaddam, A.; Mayorga-Martinez, C. C.; Sofer, Z.; Bouša, D.; Saievar-Iranizad, E.; Pumera, M. *J. Phys. Chem. C* **2017**, *121*, 20532–20538.

13. Yew, Y. T.; Sofer, Z.; Mayorga-Martinez, C. C.; Pumera, M. Black phosphorus nanoparticles as a novel fluorescent sensing platform for nucleic acid detection. *Mater. Chem. Front.* **2017**, *1*, 1130-1136.

14. Wang, L.; Sofer, Z.; Pumera, M. Voltammetry of Layered Black Phosphorus: Electrochemistry of Multilayer Phosphorene. *ChemElectroChem* **2015**, *2*, 324–327.

15. Fojtů, M.; Teo, W. Z.; Pumera, M. Environmental impact and potential health risks of 2D nanomaterials. *Environ. Sci.: Nano* **2017**, *4*, 1617–1633.

16. Latiff, N. M.; Teo, W. Z.; Sofer, Z.; Fisher, A. C.; Pumera, M. The Cytotoxicity of Layered Black Phosphorus. *Chem. Eur. J.* **2015**, *21*, 13991–13995.

17. Zhang, Z.; Xing, D.-H.; Lib, J.; Yan, Q. Hittorf's phosphorus: the missing link during transformation of red phosphorus to black phosphorus. *CrystEngComm* **2017**, *19*, 905–909.

18. Krug, H. F.; Wick, P. Nanotoxicology: an interdisciplinary challenge. *Angew. Chem. Int. Ed.* **2011**, *50*, 1260–1278.

19. Teo, W. Z.; Sofer, Z.; Sembera, F.; Janousek, Z.; Pumera, M. Cytotoxicity of fluorographene. *RSC Adv.* **2015**, *5*, 107158–107165.

20. Teo, W. Z.; Chua, C. K.; Sofer, Z.; Pumera, M. Fluorinated Nanocarbons Cytotoxicity. *Chem. Eur. J.* **2015**, *21*, 13020–13026.

21. Chng, E. L. K.; Chua, C. K.; Pumera, M. Graphene oxide nanoribbons exhibit significantly greater toxicity than graphene oxide nanoplatelets. *Nanoscale* **2014**, *6*, 10792–10797.

22. Teo, W. Z.; Chng, E. L. K.; Sofer, Z.; Pumera, M. Cytotoxicity of Exfoliated Transition-Metal Dichalcogenides (MoS_2, WS_2, and WSe_2) is Lower Than That of Graphene and its Analogues. *Chem. Eur. J.* **2014**, *20*, 9627–9632.

23. Chng, E. L. K.; Sofer, Z.; Pumera, M. Cytotoxicity Profile of Highly Hydrogenated Graphene. *Chem. Eur. J.* **2014**, *20*, 6366–6373.

24. Teo, W. Z.; Chng, E. L. K.; Sofer, Z.; Pumera, M. Cytotoxicity of halogenated graphenes. *Nanoscale* **2014**, *6*, 1173–1180.

25. Sharifi, S.; Behzadi, S.; Laurent, S.; Forrest, M. L.; Stroeve, P.; Mahmoudi, M. Toxicity of nanomaterials. *Chem Soc Rev.* **2012**, *41*, 2323–2343.

26. Bagheri, S.; Mansouri, N.; Aghaie, E. Phosphorene: A new competitor for graphene. *Int. J. Hydrogen Energy* **2016**, *41*, 4085–4095.

27. Lin, S.; Liu, S.; Yang, Z.; Li, Y.; Ng, T. W.; Xu, Z.; Bao, Q.; Hao, J.; Lee, C.-S.; Surya, C.; Yan, F.; Lau, S. P. Solution-Processable Ultrathin Black Phosphorus as an Effective Electron Transport Layer in Organic Photovoltaics. *Adv. Funct. Mater.* **2016**, *26*, 864–871.

28. Olego, D. J.; Baumann, J. A.; Kuck, M. A.; Schachter, R.; Michel, C. G.; Raccah, P. M. The microscopic structure of bulk amorphous red phosphorus: A Raman scattering investigation. *Solid State Commun.* **1984**, *52*, 311–314.

29. Lu, W. L.; Nan, H. Y.; Hong, J. H.; Chen, Y. M.; Zhu, C.; Liang, Z.; Ma, X. Y.; Ni, Z. H.; Jin, C. H.; Zhang, Z. Plasma-assisted fabrication of monolayer phosphorene and its Raman characterization. *Nano Res.* **2014**, *7*, 853–859.

30. Sofer, Z.; Bouša, D.; Luxa, J.; Mazanek, V.; Pumera, M. Few-layer black phosphorus nanoparticles. *Chem. Commun.* **2016**, *52*, 1563–1566.

31. Zaug, J. M.; Soper, A. K.; Clark, S. M. Pressure-dependent structures of amorphous red phosphorus and the origin of the first sharp diffraction peaks. *Nat. Mater.* **2008**, *7*, 890–899.

32. Baumer, F.; Ma, Y.; Shen, C.; Zhang, A.; Chen, L.; Liu, Y.; Pfister, D.; Nilges, T.; Zhou, C. Synthesis, Characterization, and Device Application of Antimony-Substituted Violet Phosphorus: A Layered Material. *ACS Nano* **2017**, *11,* 4105–4113.

33. Huang, H.; Xiao, Q.; Wang, J.; Yu, X.-F.; Wang, H.; Zhang, H.; Chu, P. K. Black phosphorus: a two-dimensional reductant for in situ nanofabrication. *npj 2D Materials and Applications* **2017**, *1*, 20, DOI:10.1038/s41699-017-0022-6.

34. Mayorga-Martinez, C. C.; Sofer, Z.; Sedmidubsky, D.; Luxa, J.; Pumera, M. Metallic impurities in black phosphorus nanoflakes prepared by different synthetic routes. *Nanoscale* **2018**, *10*, 1540–1546.

35. Jan Plutnar, Zdeněk Sofer, Martin Pumera, Products of Degradation of Black Phosphorus in Protic Solvents. *ACS Nano* **2018**, *12*, 8390–8396

36. Chng, E. L. K.; Sofer, Z.; Pumera, M. MoS_2 exhibits stronger toxicity with increased exfoliation. *Nanoscale* **2014**, *6*, 14412–14418.

37. Chng, E. L. K.; Pumera, M. The Toxicity of Graphene Oxides: Dependence on the Oxidative Methods Used. *Chem. Eur. J.* **2013**, *19*, 8227–8235.

38. Dayem, A. A.; Hossain, M. K.; Lee, S. B.; Kim, K.; Saha, S. K.; Yang, G.-M.; Choi, H. Y.; Cho, S.-G. The Role of Reactive Oxygen Species (ROS) in the Biological Activities of Metallic Nanoparticles. *Int. J. Mol. Sci.* **2017**, *18*, 120.

39. Mu, X.; Wang, J.-Y.; Bai, X.; Xu, F.; Liu, H.; Yang, J.; Jing, Y.; Liu, L.; Xue, X.; Dai, H.; Liu, Q.; Sun, Y.-M.; Liu, C.; Zhang, X.-D. Black Phosphorus Quantum Dot Induced Oxidative Stress and Toxicity in Living Cells and Mice. *ACS Appl. Mater. Interfaces* **2017**, *9*, 20399–20409.

40. Zhang, X.; Zhang, Z.; Zhang, S.; Li, D.; Ma, W.; Ma, C. X.; Wu, F.; Zhao, Q.; Yan, Q.; Xing, B. Size Effect on the Cytotoxicity of Layered Black Phosphorus and Underlying Mechanisms. *Small* **2017**, *13*, 1701210.

41. Zitka, O.; Skalickova, S.; Gumulec, J.; Masarik, M.; Adam, V.; Hubalek, J.; Trnkova, L.; Kruseova, J.; Eckschlager, T.; Kizek, R. Redox status expressed as GSH:GSSG ratio as a marker for oxidative stress in paediatric tumour patients. *Oncol. Lett.* **2012**, *4*, 1247–1253.

42. Latiff, N. M.; Sofer, Z.; Fisher, A. C.; Pumera, M. Cytotoxicity of Exfoliated Layered Vanadium Dichalcogenides. *Chem. Eur. J.* **2017**, *23*, 684–690.

43. Andersson, P. O.; Lejon, C.; Ekstrand-Hammarstrom, B.; Aktur, C.; Ahlinder, L.; Bucht, A.; Österlund, L. Polymorph- and Size-Dependent Uptake and Toxicity of TiO_2 Nanoparticles in Living Lung Epithelial Cells. *Small* **2011**, *7*, 514–523.

44. Badawy, A. M.; Silva, R. G.; Morris, B.; Scheckel, K. G.; Suidan, M. T.; Tolaymat, T. M. Surface Charge-Dependent Toxicity of Silver Nanoparticles. *Environ. Sci. Technol.* **2011**, *45*, 283–287.

45. Krug, H. F. Nanosafety Research—Are We on the Right Track? *Angew. Chem. Int. Ed.* **2014**, *53*, 12304–12319.

46. Marcano, D. C.; Kosynkin, D. V.; Berlin, J. M.; Sinitskii, A.; Sun, Z.; Slesarev, A.; Alemany, L. B.; Lu, W.; Tour, J. M. Improved Synthesis of Graphene Oxide. *ACS Nano* **2010**, *4*, 4806–4814.

47. Kang, J. H.; Kim, T.; Choi, J.; Park, J.; Kim, Y. S.; Chang, M. S.; Jung, H.; Park, K. T.; Yang, S. J.; Park, C. R. Hidden Second Oxidation Step of Hummers Method. *Chem. Mater.* **2016**, *28*, 756−764.